

Original Research

Temporal-Spatial Variations of Concentrations of PM₁₀ and PM_{2.5} in Ambient Air

Liu Jie^{1,2}, Hou Kepeng^{1,2}, Wang Xiaodong^{1,2*}, Yang Peng³

¹Faculty of Land and Resources Engineering, Kunming University of Science and Technology, Kunming, China

²Postdoctorate Station of Mining Industry Engineering, Kunming University of Science and Technology, Kunming, China

³Beijing Key Laboratory of Information Service Engineering, Beijing Union University, Beijing, China

Received: 3 April 2016

Accepted: 11 June 2016

Abstract

Since the space points' average concentrations of PM obtained by air quality automatic monitoring sites were less representative of PM pollution levels in the Beijing area, it was necessary to improve the spatial resolution of PM concentrations on the basis of continuous time series. In order to solve the problem, we used one-hour average concentrations of PM from March 2013 to February 2014 obtained by monitoring sites. Firstly, concentration variations with time scale of PM_{2.5} and PM₁₀ were researched to find out their correlations and pollution grades in continuous time series. Secondly, in order to realize the spatial distribution characteristics from points to surfaces, MATLAB spatial interpolation tools were used to predict the average concentrations of PM on any latitude-longitude grid in regional surface, then spatial interpolation on longitudes and latitudes, and the PM concentrations were researched by radial basis functions based on biharmonic green function. Finally, by constructing decision functions and sample sets, the interpolation results were tested by *k*-fold cross validation to analyze the error distribution between monitoring values and fitted values, and then they were compared with Kriging interpolation results realized by DACE tool in MATLAB. The results showed there were periodical variations and significant correlations on the average concentrations of PM from March 2013 to February 2014 in Beijing. The PM pollutions also had obvious regional characteristics. Interpolation results of radial basis function interpolation on PM concentrations could represent their spatial distribution in Beijing, since the method had a certain precision to improve utilization of spatial information. Moreover, the analysis showed that the main factors of PM pollution were dust storms and strong winds in spring and autumn, rainfall and the warm wet climate in summer, and cold fronts and snowfall in winter. Pollution characteristics in the Beijing area were higher in the south and lower in the north, and the pollution sources might be regional transport as well as local anthropogenic sources. The conjoint analysis on time series and spatial interpolation of concentrations had significance for further research of time-space relationship of PM, and it also provided a method for understanding regional pollution characteristics.

Keywords: atmospheric pollution, particulate matters, concentration, temporal-spatial variation, interpolation

Introduction

Rapid economic development has recently aggravated environmental pollution [1-23]. Atmospheric pollution in Beijing and the surrounding area have appeared to include remarkably regional and compound characteristics, with particulate matters (PM) being the key factors resulting in these pollution characteristics [4]. $PM_{2.5}$ and PM_{10} pollution would not only directly affect human health but also cause a decrease of visibility on a regional scale, and even affect climate change during their transmission [5-8]. Research on PM pollution characteristics and their temporal-spatial variation could obtain macroscopic pollution trends and provide a reference to realize their distribution in each region. At present, PM pollution characteristics are mainly researched by the method of spatial scale and time scale. The spatial scale method used satellite image interpretation in general [9], which was higher in spatial resolution but was incomplete in the time series, and there were also uncertainty errors in this method caused by geographic elevation, clouds, and light reflex. The time-scale method used a certain number of monitoring points established to realize data observation and sampling [10], which was complete in time series but lower in spatial resolution, and we were unable to obtain the pollutant concentrations outside the monitoring points in other regions. In addition, spatial distribution characteristics of PM were usually analyzed by a sole monitoring point and it was hard to provide sufficient evidence of regional representatives and their ranges. In order to represent regional pollution by limited ground monitoring sites, spatial interpolation was still an effective method widely used in environmental areas [11-12]. However, the research objects of spatial interpolation were mainly in soil elements [13-14] and meteorological elements [15-16], and less in atmospheric PM due to a certain number of samples being required for this method. Due to objective reasons such as the incomplete monitoring system and the high-cost of atmospheric monitoring equipment over a long period of time, it was difficult to obtain PM concentrations with the same complete time series in multiple points.

The air quality automatic monitoring network that covered the Beijing area had not been established until January 1, 2012. Six pollutants, including $PM_{2.5}$ and PM_{10} and gaseous pollutants (CO , SO_2 , O_3 , and NO_2) could be continuously monitored and their time series are complete. Based on this, there are larger samples for researching PM pollution and distribution characteristics. It was known that PM in different regions were not independent of each other, so the PM average concentrations and their distribution laws in the whole region surface could be explored and predicted by analyzing the concentrations obtained by different monitoring sites. One-hour PM average concentrations from March 2013 to February 2014 obtained by air quality monitoring sites were used to analyze the concentration variations of PM with time scales and their significant correlations. Then regional distribution diagrams of quarterly average concentrations of $PM_{2.5}$ and PM_{10} were realized to describe the spatial

distribution of PM and their local pollution characteristics by the high-dimensional spatial interpolation method in the MATLAB tool. In addition, the quarterly average concentrations of PM on any latitude-longitude grid were fitted. Finally, the difference between fitted values and actual values were tested to verify the feasibility and accuracy of the method. Through the above methods, the average concentration variations of PM in different time periods could be found out and the PM pollution characteristics from points to surfaces realized. This provided a method for predicting spatial distribution of PM and realizing their visualization.

Experimental

In order to understand air quality of the Beijing area, the air quality automatic monitoring network included 35 sites as established by the Beijing Municipal Environmental Monitoring Center. The monitoring network is divided into urban or suburban evaluation sites, control or background sites, and traffic sites. Among them, urban or suburban evaluation sites are used to monitor air quality trends and typical concentrations in an environment quality functional zone. Control or background sites are used to monitor air quality without pollution-immune in a local city. Traffic points are used to monitor the traffic pollution effect on ambient environment. All 35 sites are distributed throughout six urban and ten suburban areas to represent air quality of the whole Beijing area. The distribution of auto monitoring sites and names as well as their administrative region are shown in Fig. 1 and Table 1, respectively.

The data obtained by automatic air quality monitoring sites were the time statistics to represent pollutant concentrations somewhere in the ground layer. In order

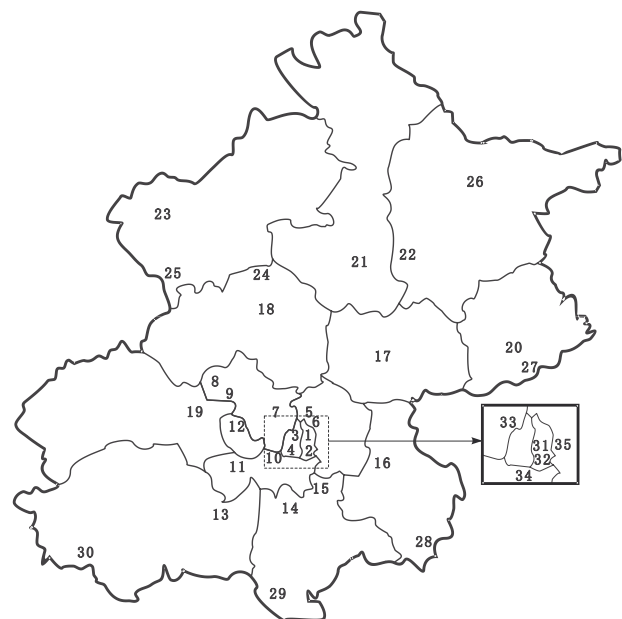


Fig. 1. Air quality automatic monitoring sites in Beijing.

Table 1. Site names and their functions.

Site	Name	Function	Site	Name	Function	Site	Name	Function
1	Dongsi	Evaluation	13	Fangshan	Evaluation	25	Badaling	Background
2	Temple of Heaven	Evaluation	14	Daxing	Evaluation	26	Miyun reservoir	Background
3	Guanyuan	Evaluation	15	Yizhuang	Evaluation	27	Donggaocun	Background
4	West Wanshou Nishinomiya	Evaluation	16	Tongzhou	Evaluation	28	Yongledian	Background
5	Olympic Sports Center	Evaluation	17	Shunyi	Evaluation	29	Yufa	Background
6	National Agricultural Exhibition Center	Evaluation	18	Changping	Evaluation	30	Liulihe	Background
7	Wanliu	Evaluation	19	Mentougou	Evaluation	31	West Qianmen	Traffic
8	Northern new area	Evaluation	20	Pinggu	Evaluation	32	Inner Yongdingmen	Traffic
9	Botanical Garden	Evaluation	21	Huairou	Evaluation	33	North Xizhimen	Traffic
10	Fengtai garden	Evaluation	22	Miyun	Evaluation	34	South 3rd Ring Rd	Traffic
11	Yungang	Evaluation	23	Yanqing	Evaluation	35	East 4rd Ring Rd	Traffic
12	Gucheng	Evaluation	24	Dingling	Control			

Note: Sites 1-12 are urban evaluation points in and sites 13-23 are suburban evaluation points.

to research the pollution characteristics of PM and their spatial distribution, one-hour average real-time monitoring values of PM concentrations at 35 sites were collected from March 2013 to February 2014. There were 24 groups of one-hour average concentrations of $PM_{2.5}$ and PM_{10} per day (data loss occurred in part time) per point. Moreover, the data were treated as follows: 1) calculating 24-hour and one-quarter average concentrations of $PM_{2.5}$ and PM_{10} at each monitoring site and 2) calculating 24-hour and one-quarter average concentrations of $PM_{2.5}$ and PM_{10} of 35 monitoring sites, which represented the average concentrations for Beijing.

Results and Discussion

Time Variation Characteristics

The 24-hour average mass concentration variations from March 2013 to February 2014 are shown in Figs 2a-d. It could be seen there was obvious periodicity (5-7 days) of PM concentrations, which were similar to the pattern of bimodal parabolic and main as decided by the seasonal weather [17]. Meteorological conditions [18] such as temperature, wind speed and solar radiation could influence the PM concentrations. According to the actual meteorological conditions, the PM concentrations in early spring 2013 were relatively high in the unfavorable diffusion of weather, which was caused by continuous low temperatures. Fig. 2a) shows the average concentrations of $PM_{2.5}$ and PM_{10} as being high in early spring, and both of their variation trends were consistent. The wave crests of concentrations (serious pollution) in March 17 and March 26 were caused by the transit of

the cold front as well as the dust weather. The obvious decline of PM concentrations after March 18 might be caused by cold air activity in snowy weather with low relative humidity, which could make for better diffusion conditions for diluting PM [19]. The second wave crests of PM concentrations in mid- to late spring might also be connected with the dust weather in that time period. There was obvious decline on $PM_{2.5}$ average concentration in late April and early May, and it was down 40.7% in April over March. PM_{10} average concentration slightly declined but was still in a high level caused by sustained high winds. According to actual wind meteorological data from April 1 to May 31 from the Beijing Meteorological Bureau, 33 days of wind speed were above grade 4 (3.4-5.4 m/s) and eight days were above grade 5 (8.0-10.7m/s), mainly in April. The previous research showed that high winds had a better effect in $PM_{2.5}$ purification, but the concentration of PM_{10} would increase with the increased wind speed when above grade 2 [20].

The variation trend of PM concentrations in May was similar to the concentrations in April, but the average concentrations of $PM_{2.5}$ and PM_{10} increased 24.4% and 21.5%, respectively. Figure 2b) shows higher PM concentrations in early to mid summer, which were connected with the unfavorable diffusion weather caused by warm moisture and the decline of wind speed. There was hot weather with fog and haze pollution (heavy pollution) on May 6 and June 28, which might be caused by the secondary formation of O_3 due to the increase of sunshine and temperature. The concentrations of $PM_{2.5}$ and PM_{10} declined in the consistent rainfall after May 7 and June 30, with the removal efficiency of 45.6%-67.1 in previous research [16]. However, the air relative humidity before or after rainfall would result in unfavorable conditions of

Table 2. Concentration limits of PM and corresponding individual air quality indexes.

24-hour average concentration/ $\mu\text{g}\cdot\text{m}^{-3}$		IAQI	Grade	Effects on human health
PM _{2.5}	PM ₁₀			
0-35	0-50	0-50	1: Excellent	Air quality is satisfactory with almost no pollution
36-75	51-150	51-100	2: Good	Air quality is acceptable, but some pollutants may impact sensitive groups
76-115	151-250	101-150	3: Mild pollution	Symptoms of sensitive groups are mildly intensified and health groups incur irritative symptoms
116-150	251-350	151-200	4: Moderate pollution	Symptoms of sensitive groups are further intensified, health groups' heart and respiratory systems may be affected
151-250	351-420	201-300	5: Heavy pollution	Symptoms of cardiopath and lungers are significantly intensified and tolerance decreases; most general health groups experience symptoms
251-500	421-600	>300	6: Serious pollution	Exercise tolerance of health groups decrease and symptoms of them are strong; some diseases will appear earlier

spread, causing an increase of PM concentrations. The fluctuant change of PM concentrations in late May and late June might also be connected with the frequent rainfall in that time period. The changes of PM concentrations were stable from July 2 to September 24, and this was connected with the dry clean air in Summer. There were still obvious periodic oscillations but its state was more stable.

Fig. 2c) shows a sharp increase in PM concentrations from September 25 to November 25, which was more fluctuant than in spring. The reason for the above appearance might be connected with meteorological factors similar to the ones in spring. Fig. 2d) shows PM concentrations at a high level, which was connected with the stable climate in winter. Moreover, the variation ranges and rangeabilities of PM concentrations were larger in late winter – especially the wave crest of concentrations generated in mid-January and late February 2014. According to the pollution process, there was fog and haze pollution in January 16 (heavy pollution), and after that snowfall arrived and the PM were obviously removed. The meteorological data from February 13 to February 28 also reported two snowfall days (February 13 and February 18), one rainfall day (February 26), two clear weather

days (February 19 and February 27), and other days of serious fog and haze pollution, so these days caused the sharp increase and sharp fluctuation of PM concentrations. In addition, from three serious pollution days in winter (24-hour average concentration of PM_{2.5} was above 250 $\mu\text{g}\cdot\text{m}^{-3}$), there were two fog and haze pollution days (December 7 and December 24) and one cloudy weather day (January 23), so serious PM pollution was caused by the stable meteorological conditions and other factors together.

Concentration limits of PM and their corresponding individual air quality index (IAQI) grades of Chinese national standards are shown in Table 2. The 24-hour average concentration limits of PM_{2.5} in the second environment functional area such as a residential area is 75 $\mu\text{g}\cdot\text{m}^{-3}$, while PM₁₀ is 150 $\mu\text{g}\cdot\text{m}^{-3}$ [21]. In 356 days from March 2013 to February 2014, the variation range of 24-hour average concentrations of PM_{2.5} was 7.42-407.6 $\mu\text{g}\cdot\text{m}^{-3}$ while the average value was 92.1 $\mu\text{g}\cdot\text{m}^{-3}$. There were 170 days of 24-hour average concentrations above 75 $\mu\text{g}\cdot\text{m}^{-3}$ and the control rates were 52.2%. The variation range of 24-hour average concentrations of PM₁₀ was 12.1-405.7 $\mu\text{g}\cdot\text{m}^{-3}$ while the average value is

Table 3. Concentration variation and pollution grade of PM.

Season	PM	Minimum daily average value / $\mu\text{g}\cdot\text{m}^{-3}$	Maximum daily average value / $\mu\text{g}\cdot\text{m}^{-3}$	Quarterly average value / $\mu\text{g}\cdot\text{m}^{-3}$	Concentration ratio $\rho(\text{PM}_{2.5})/\rho(\text{PM}_{10})$ /%	Pollution grade
Spring	PM _{2.5}	13.4	179.6	84.4	70	3: Mild pollution
	PM ₁₀	29.4	222.7	120.0		
Summer	PM _{2.5}	9.0	297.1	79.7	79.3	3: Mild pollution
	PM ₁₀	27.1	317.0	100.8		
Autumn	PM _{2.5}	7.4	299.0	87.7	77.8	3: Mild pollution
	PM ₁₀	18.8	318.2	111.9		
Winter	PM _{2.5}	5.9	407.6	116.4	87.7	4: Moderate pollution
	PM ₁₀	12.1	405.7	132.8		

Table 4. Regression and correlation analysis of concentrations of PM_{2.5} and PM₁₀ ($y = ax + b$).

Season	Slope a	Intercept b	Correlation coefficient R	Goodness of fit R^2	Degree of freedom $n-2$	Significance level α	
						$R_{0.05}$	$R_{0.01}$
Spring	0.84	-10.07	0.80	0.64	80	0.217	0.283
Summer	0.92	-13.10	0.93	0.86	90	0.205	0.267
Autumn	0.97	-22.38	0.97	0.94	89	0.205	0.267
Winter	0.96	-11.85	0.97	0.94	88	0.205	0.267

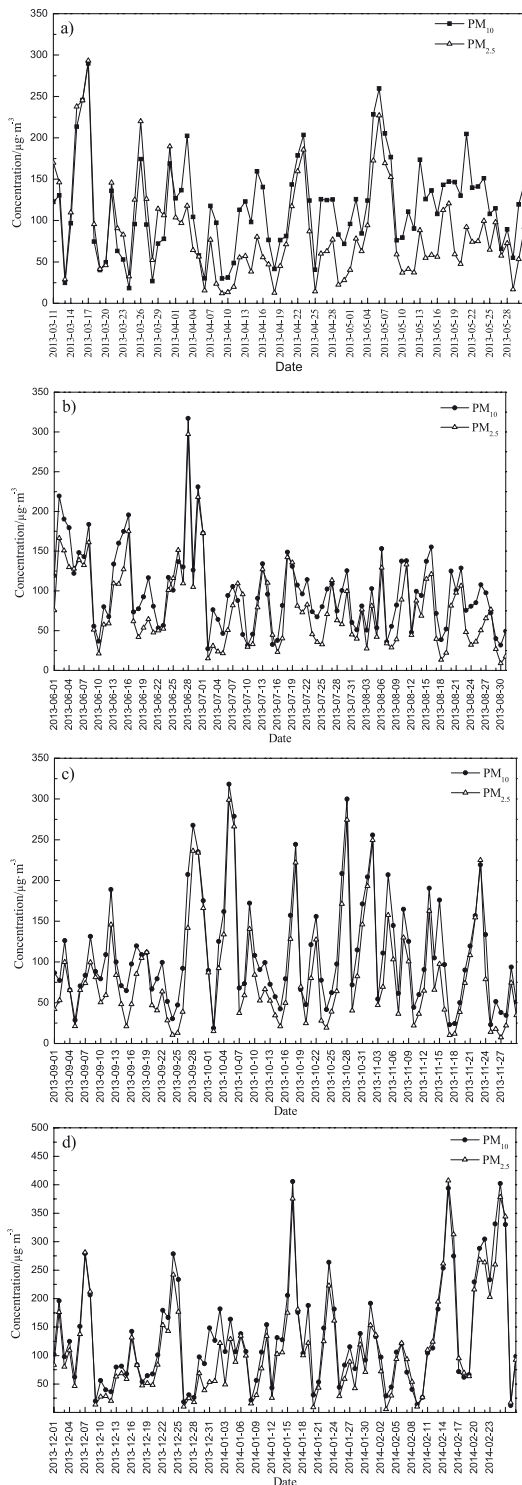


Fig. 2. Concentration variations of PM with time scale.

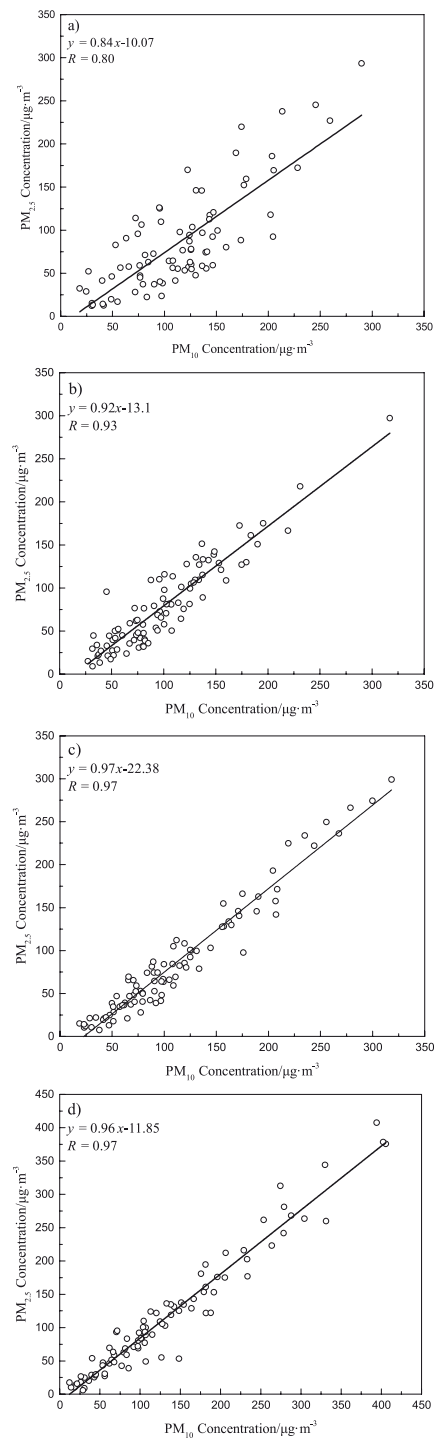


Fig. 3. Correlation analysis on quarterly average concentrations of PM_{2.5} and PM₁₀.

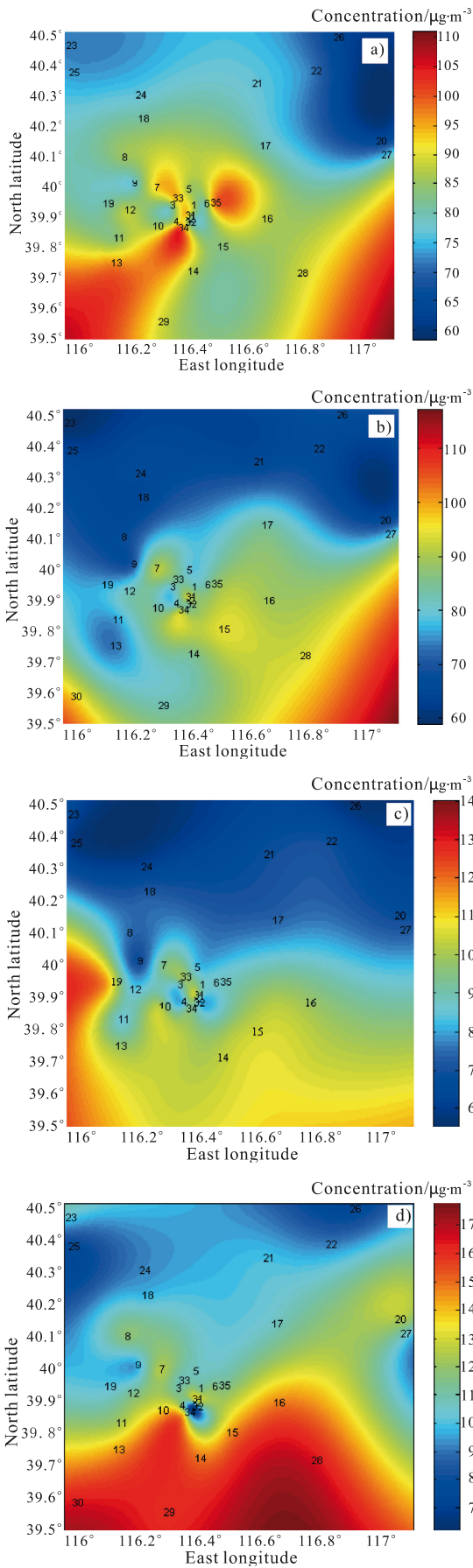


Fig. 4. Interpolation of quarterly average concentration and geographical distribution of $PM_{2.5}$ in Beijing, March 2013 to February 2014.

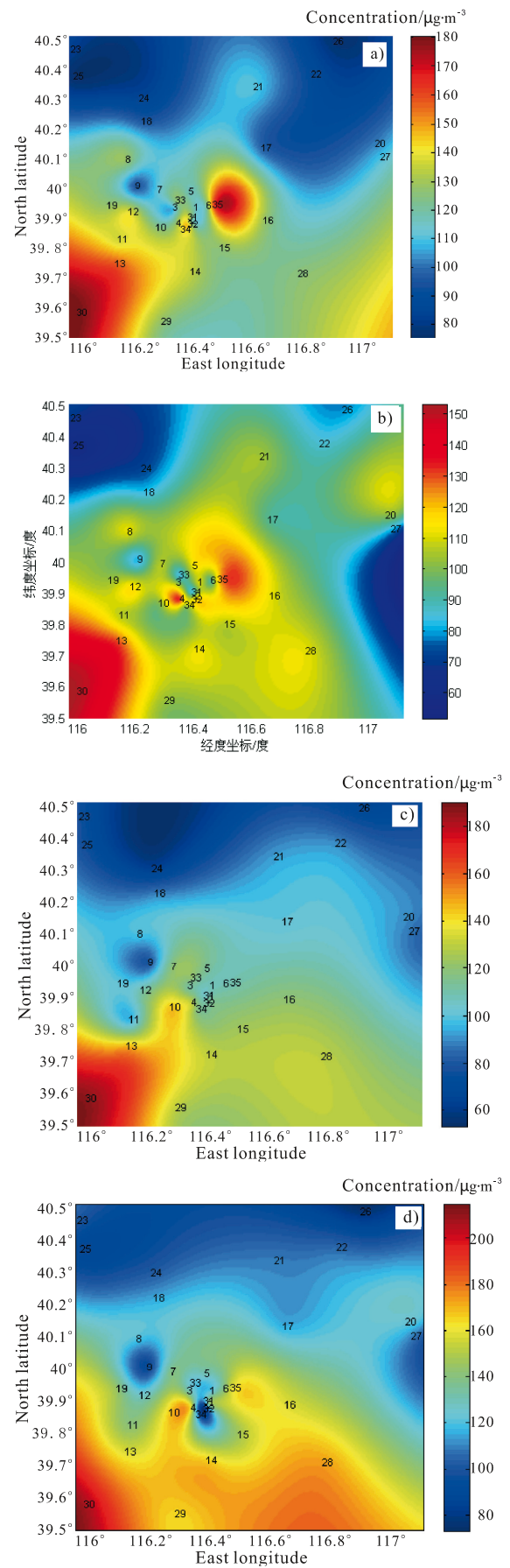


Fig. 5. Interpolation of quarterly average concentration and geographical distribution of PM_{10} in Beijing, March 2013 to February 2014.

116.4 $\mu\text{g}\cdot\text{m}^{-3}$. There were 81 days of 24-hour average concentrations above 150 $\mu\text{g}\cdot\text{m}^{-3}$, and the control rate of 24-hour average concentrations is 77.2%. The maximum of 24-hour average concentrations of PM_{10} and $\text{PM}_{2.5}$ appeared in spring (January 16 and February 25), and the maximum of 24-hour average concentrations of PM_{10} and $\text{PM}_{2.5}$ appeared in autumn (October 2 and November 17). The concentration variation and pollution grade of PM are shown in Table 3.

Figs 3a-d) show our analysis of the correlations of quarterly average concentrations of $\text{PM}_{2.5}$ and PM_{10} obtained by 35 monitoring stations. There was a linear relationship between $\text{PM}_{2.5}$ and PM_{10} regarding their quarterly average concentrations. The linear regression and correlation analysis results in Table 4 showed that the correlation coefficient R of PM concentrations in four seasons from March 2013 to February 2014 were 0.80, 0.93, 0.97, and 0.97, respectively. Since $0 < |R| < 1$ and in condition of significance level $\alpha = 0.01$, there was a significant liner relation between $\text{PM}_{2.5}$ and PM_{10} on their concentrations due to $R \square R_{0.01}$.

Regional Distribution Characteristics

By using the spatial interpolation method on average concentrations of PM at monitoring sites, the concentration distribution characteristics of PM pollution in Beijing could be further visualized. Moreover, the quarterly average concentrations of the entire interpolation surface could be predicted. Spatial interpolation is a method to extrapolate any point data or regional data by the given data. Using this method the concentrations of PM on any corresponding latitude-longitude of regional surface could be fitted. The radial basis function was used to realize interpolation, which was not necessary for predicting the spatial variance structure. Moreover, the statistical hypothesis from these sources are difficult to estimate and verify. Keeping certain precision, this method also has the advantages of being easily programmable and requiring less calculation [21].

According to the latitude-longitude range of Beijing and the distribution of 35 monitoring sites, we selected the geospatial range of 39.5-40.5 degrees north latitude, 116-117.2 degrees east longitude, which covered most region of Beijing. The spatial interpolation function in the MATLAB tool was used, whose algorithm implementation about radial basis function was mainly based on the biharmonic green function [22]. This algorithm is a minimum curvature interpolation, with the interpolation surface constructed by the liner combination of green function with each sampling point as the center by adjusting the weights of each sampling point so that the surface could through all of them. Since the number of green functions could be less than the number of data points, the interpolation curve would not be matched with inaccurate data points. In a three-dimensional space constructed by latitude-longitude coordinates and particulate concentrations, the mesh collections composed by curves were the desired surface, so each curve represented the longitude-latitude grids

and their corresponding concentrations on one section. The results of dividing the longitude and latitude of the research region into 200×200 grids, then using quarterly average concentrations of $\text{PM}_{2.5}$ and PM_{10} obtained by 35 monitoring sites from March 2013 to February 2014 and their corresponding longitude-latitude coordinates for spatial interpolation are shown in Figs 4a-d and 5a-d

In order to validate the veracity, k -fold cross validation was used for interpolation results disproof, and then they were compared with the results obtained by Kriging interpolation. We divided 35 interpolation objects into seven sets randomly, with six sets (30 points) for interpolation to get a decision function and one set (5 points) for sample validation by decision function. We started with validating the seven repetitions and the average test error of them were the generalization error. Then we evaluated the fitting results by calculating their mean errors (ME), mean absolute errors (MAE), root mean square errors (RMSE), and mean relative errors (MRE). Among them, ME reflected the total error magnitude of estimated values, MAE reflected the probable error range of estimated values, RMSE reflected the inversion sensitivity and extreme values effect of interpolation function, and MRE reflected precision discretion.

$$\delta_{ME} = \frac{\sum_{i=1}^n (C_i - \hat{C}_i)}{n} \tag{1}$$

$$\delta_{MAE} = \frac{\sum_{i=1}^n |C_i - \hat{C}_i|}{n} \tag{2}$$

$$\delta_{RMSE} = \sqrt{\frac{\sum_{i=1}^n (C_i - \hat{C}_i)^2}{n}} \tag{3}$$

$$\delta_{MRE} = \frac{\sum_{i=1}^n \left| \frac{C_i - \hat{C}_i}{C_i} \right|}{n} \tag{4}$$

...where δ_{ME} , δ_{MAE} , δ_{RMSE} , and δ_{MRE} were ME, MAE, RMSE, and MRE between the actual monitoring values C_i and fitting values \hat{C}_i , respectively; n was the number of monitoring sites.

Take the cross-validation interpolation results of quarterly $\text{PM}_{2.5}$ concentrations (in spring) of 35 monitoring sites in Beijing, for example. Table 5 shows how we divided the 35 points into groups ①-⑦ using the MATLAB random function.

Firstly, group ① $C_{1p} = \{77.48, 97.25, 76.93, 79.06, 94.11\}$ was chosen to be a validation set and the remaining groups ②-⑦ $C_p = \{C_{2p}, C_{3p}, C_{4p}, C_{5p}, C_{6p}, C_{7p}\}$ were chosen to be the test sets. Then the corresponding fitted values in longitude-latitude coordinates that were matched with group ① could be found and the result was

Table 5. Groups for *k*-fold cross validation.

Grouping	①	②	③	④	⑤	⑥	⑦
Site number	9	2	3	8	18	1	6
	13	4	17	12	20	7	10
	24	5	23	14	26	21	15
	25	11	28	19	30	22	16
	27	29	34	32	33	25	31

$\hat{C}_{1p} = \{85.5, 88.7, 77.3, 69.5, 82.3\}$. Finally, the remaining six groups were chosen to be validation sets and test sets, and the cyclic calculation would not be stopped until all groups were chosen once. According to the quarterly $PM_{2.5}$ concentrations obtained (in spring), the sample matrix based on actual monitoring values of groups and their corresponding fitted values could be constructed as follows:

$$C_{mp} = \begin{bmatrix} \textcircled{1} & \textcircled{2} & \textcircled{3} & \textcircled{4} & \textcircled{5} & \textcircled{6} & \textcircled{7} \\ 77.5 & 82.2 & 80.9 & 84.8 & 81.1 & 88.2 & 81.8 \\ 97.3 & 87.8 & 80.2 & 87.8 & 67.1 & 92.1 & 86.5 \\ 76.9 & 87.0 & 72.0 & 87.8 & 64.7 & 76.9 & 83.0 \\ 79.1 & 83.8 & 88.5 & 80.3 & 104.7 & 71.5 & 87.8 \\ 94.1 & 89.3 & 102.8 & 88.0 & 93.2 & 73.4 & 93.1 \end{bmatrix};$$

$$\hat{C}_{mp} = \begin{bmatrix} \textcircled{1} & \textcircled{2} & \textcircled{3} & \textcircled{4} & \textcircled{5} & \textcircled{6} & \textcircled{7} \\ 85.5 & 93.8 & 90.8 & 77.3 & 82.7 & 83.7 & 91.9 \\ 88.7 & 86.4 & 90.8 & 77.5 & 76.9 & 83.7 & 89.4 \\ 77.3 & 97.7 & 73.0 & 98.0 & 75.4 & 70.7 & 88.8 \\ 69.5 & 91.4 & 87.4 & 73.2 & 104.7 & 61.7 & 89.0 \\ 82.3 & 98.7 & 84.7 & 93.4 & 87.1 & 73.4 & 73.2 \end{bmatrix}$$

Putting the actual monitoring values of groups and their corresponding fitted values into equations (1)-(4) and the results showed that δ_{ME} was -0.1, δ_{MAE} was 7.35, δ_{RMSE} was 8.74% and δ_{MRE} was 6.89%. Similarly, the cross validations of average concentration interpolation of $PM_{2.5}$ and PM_{10} in other seasons could be calculated in the sequence shown in Table 6. In addition, in order to contrast the effects of different interpolation methods, Kriging

interpolation was used by DACE tools in MATLAB and their results (validated by the method above) are shown in Table 7.

Tables 6 and 7 showed that the effects of two interpolation methods were similar and both of them had certain accuracies. Both have poor interpolation effects on PM_{10} concentrations because there was great regional variability on monitoring data, so that there were significant differences between a few points and their adjacent points, which caused an overly idealized deviation in spatial interpolation, so the fitting results could not reflect the truth of the surface. The error of Kriging interpolation occurred in the models and its complicated parametric optimization, as well as the algorithm implementation of software and its completeness on optimal fitting parametrics of the Kriging function. The different interpolation algorithms on different research objects required analysis and evaluations according to the actual conditions. In addition, the same interpolation algorithms on different PM concentrations in different times might have different interpolation effects. Cross validations showed that the radial basis function based on the biharmonic green function were better, with the average MRE of interpolation of $PM_{2.5}$ and PM_{10} being 10.69% and 21.26%, respectively. This method was a better option because of its easy operation and calculation, and its fitted results had certain representativeness.

Figs 4a-d and 5a-d show obvious regional characteristics for PM concentrations, and their frequency distribution could also be obtained. In Fig. 4a, for example, the high frequency distribution range of $PM_{2.5}$ concentration was 60-110 $\mu g \cdot m^{-3}$ in the Beijing area. Among them, the urban areas were in long-term $PM_{2.5}$ mild pollution. In suburbs, the polluted area was Fangshan (mild to moderate pollution of $PM_{2.5}$ in the long term) and the least polluted area was Miyun (good in the long term). The Miyun Reservoir could represent the characteristics of the clean air of northeastern Beijing. Overall, $PM_{2.5}$ pollution was the main pollution and most of the areas were in pollution of different degrees. The pollution characteristics of the Beijing area were higher in the south and lower in the north. Compared with the results from 2007 [10], there was no obvious change in pollution characteristics in Beijing during these years. The $PM_{2.5}$ pollution in urban areas was affected by meteorological factors as well as artificial sources. On the other hand, PM pollution in suburb areas might be derived from regional transport.

Table 6. Cross validation results of radial basis interpolation.

Season	$PM_{2.5}$				PM_{10}			
	ME	MAE	RMSE	MRE/%	ME	MAE	RMSE	MRE/%
Spring	0.1	7.35	8.73	8.74	4.45	18.63	24.44	14.93
Summer	-0.08	7.17	8.45	9.65	-2.96	24.18	26.61	26.59
Autumn	-3.81	8.51	10.55	11.74	-5.88	23.10	25.31	25.17
Winter	-12.36	13.45	18.36	12.63	-14.8	18.47	22.62	18.36
Average	-4.04	9.12	11.52	10.69	-4.79	21.10	24.75	21.26

Table 7. Cross-validation results of Kriging interpolation.

Season	PM _{2.5}				PM ₁₀			
	ME	MAE	RMSE	MRE/%	ME	MAE	RMSE	MRE/%
Spring	3.43	8.40	8.96	9.69	5.20	24.40	27.73	20.06
Summer	-4.54	7.21	7.90	10.00	2.06	32.49	34.57	34.70
Autumn	-8.26	15.08	16.11	21.11	-9.05	30.63	33.41	35.01
Winter	-17.75	25.71	25.90	24.71	-21.78	26.59	29.07	26.24
Average	-6.78	14.1	14.72	16.38	-5.89	28.52	31.20	29.00

For instance, serious PM pollution in southern areas was affected not only by industrial dust, meteorology, and topography in this locality, but also by transportation from the surrounding provinces and cities such as Hebei, Tianjin, and Shandong. Especially given the effect of the southern wind, the contribution rate of transportation from Hebei could reach 50-70% [23]. However, the degree of influence of regional transport should be further observed and analyzed to provide sufficient evidence.

Conclusions

The concentration data of PM₁₀ and PM_{2.5} from March 2013 to February 2014 in Beijing obtained by 35 monitoring sites was a continuous time sequence. According to the quarterly average concentrations in four seasons, there was long-term mild pollution in spring, summer, and autumn, and moderate pollution in winter. The yearly standard-reaching rates of PM₁₀ and PM_{2.5} were 52.2% and 77.2%, and there were significant linear correlations between them with the correlation coefficients of 0.8, 0.93, 0.97, and 0.87. According to the spatial interpolation in MATLAB tools and the cross-validation of the results, the interpolation effects of either radial basis function or Kriging were similar. The radial basis function based on the biharmonic green function had the advantages of easy operation and smaller calculation, and its minimum curvature interpolation could obtain a smooth-fitting surface so that high accuracy could then be obtained when the spatial variability was lower. The results showed there were obvious PM regional pollution characteristics in Beijing that the different areas were in PM pollution of different degrees. By using the spatial interpolation method, the average concentrations of PM in any latitude-longitude grid of the Beijing area could be predicted, so that the local, discrete, and limited point source data could be translated to regional surface distribution and the spatial resolution of monitoring results were improved. This method had extensive application prospects in the research of PM concentration distributions. But further research was necessary for selecting and verifying the interpolation function. And the results of satellite retrieval in a certain period of time could be used to verify its accuracy. PM pollution in Beijing was an involved problem in that its pollution characteristics were affected by local emissions, meteorology, geography, and other unknown factors.

There were certain periodical and regional PM average concentrations during the period from March 2013 to February 2014. The PM concentrations were affected by seasonal variation and meteorological factors from late winter to early summer, including dust storms and strong winds in spring and autumn, rainfall and warm wet climate in summer, and a cold front and snowfall in winter. The pollution characteristics were higher in the south and lower in the north. The PM pollution in urban areas might be mainly affected by anthropogenic sources, while the serious pollution areas in the southern suburbs might be derived from regional transport.

Acknowledgements

This research is supported by China postdoctoral science foundation projects (2016M592895XB, 2015M582779XB) and the importation and development of high-caliber talent projects of Beijing municipal institutions (CIT and TCD20130320).

References

1. CETIN M. A Change in the Amount of CO₂ at the Center of the Examination Halls: Case Study of Turkey. *Ethno Med.* **10** (2), 146, **2016**.
2. CETIN M., SEVIK H. Measuring the Impact of Selected Plants on Indoor CO₂ Concentrations. *Polish Journal of Environmental Studies.* **14** (6), 781, **2005**.
3. SEVIK H., CETIN M., BELKAYALI N. Effects of Forests on Amounts of CO₂: Case Study of Kastamonu and Ilgaz Mountain National Parks. **24** (1), 253, **2015**.
4. YANG L.X., ZHOU X.H., WANG Z., ZHOU Y., CHENG S., XU P.J., GAO X.M., NIE X.F., WANG X.F., WANG W. X. Airborne fine particulate pollution in Jinan, China: Concentrations, chemical compositions and influence on visibility impairment. *Atmospheric Environment.* **55**, 506, **2012**.
5. QIU H., YU I.T., TIAN L.W., WANG X.R., TSE L.A., TAM W., WONG T.W. Effects of coarse particulate matter on emergency hospital admissions for respiratory diseases: a time-series analysis in Hong Kong. *Environmental Health Perspectives.* **120** (4), 572, **2012**.
6. LEPEULE J., LADEN F., DOCKERY D., SCHWARTZ J. Chronic Exposure to Fine Particles and Mortality: An Extended Follow-up of the Harvard Six Cities Study from 1974 to 2009. *Environmental Health Perspectives.* **120** (7), 965, **2012**.

7. KAZIL J., STIER P., ZHANG K., QUAAS J., O'DONNELL D., RAST S., ESCH M., FERRACHAT S., LONHMANN J., FEICHTER J. Aerosol nucleation and its role for clouds and Earth's radiative forcing in the aerosol-climate model ECHAM5-HAM. *Atmospheric Chemistry and Physics*. **10** (22), 10733, **2010**.
8. ZHANG K., DONNELL D.O., KAZIL J., STIER P. The global aerosol-climate model ECHAM-HAM, version 2: sensitivity to improvements in process representations. *Atmospheric Chemistry and Physics*. **12** (3), 8911, **2012**.
9. AARON V.D., RANDALL V.M., MICHAEL B.,RALPH K., ROBERT L., CAROLYN V., PAUL J.V. Global estimates of ambient fine particulate matter concentrations from environment satellite-based aerosol optical depth: development and application. *Environment Health Perspectives*. **118** (6), 847, **2010**.
10. ZHAO Q., HE K.B., MA Y.L., JIA Y.T., CHEN Y., LIU H., WANG S.W. Regional PM pollution in Beijing and surrounding area during summertime. *Environmental Sciences*. **30** (7), 1873, **2009**.
11. MONTERO J.M., CHASCO C. Building an environmental quality index for a big city: a spatial interpolation approach combined with a distance indicator. *Journal of Geographical Systems*. **12** (4), 435, **2010**.
12. LI J., HEAP A.D. A review of comparative studies of spatial interpolation methods in environmental sciences: performance and impact factors. *Ecological Informatics*. **6** (3-4), 228, **2011**.
13. XIE Y., CHEN T., LEI M., YANG J., GUO Q.J., SONG B., ZHOU X.Y. Spatial distribution of soil heavy metal pollution estimated by different interpolation methods: Accuracy and uncertainty analysis. *Chemosphere*. **82** (3), 468, **2011**.
14. DAVIS T.H., AELION M., MCDERMOTT S., LAWSON A.B. Identifying natural and anthropogenic sources of metals in urban and rural soils using GIS-based data, PCA, and spatial interpolation. *Environmental Pollution*. **157** (8-9), 2378, **2009**.
15. HOFSTRAN., NEW M., MCSWEENEY C. The influence of interpolation and station network density on the distributions and trends of climate variables in gridded daily data. *Climate Dynamics*. **35** (5), 841, **2009**.
16. AALTO J., PIRINEN P., HEIKKINEN J.,VENALAINEN A. Spatial interpolation of monthly climate data for Finland: comparing the performance of kriging and generalized additive models. *Theoretical and Applied Climatology*. **112** (1), 99, **2013**.
17. HE K.B., JIA Y.T., MA Y.L., LEI Y., ZHAO Q., TANAKA S., OKUDA T. Regionality of episodic aerosol pollution in Beijing. *Acta Scientiae Circumstantiae*, **29** (3), 482, **2009**.
18. TAI A. P.K., MICKLEY L.J., JACOB D.J. Correlations between fine particulate matter (PM_{2.5}) and meteorological variables in the United States: Implications for the sensitivity of PM_{2.5} to climate change. *Atmospheric Environment*. **44** (32), 3976, **2010**.
19. PAN B.F., ZHAO Y.L., LI J.J., WANG R.B. Analysis of the scavenging efficiency on PM_{2.5} concentration of some kinds of meteorological factors. *Environmental Science and Technology*. **25** (6), 41, **2012**.
20. WANG Y., LIU Y.P., LI J., B., LIU L.T. The effect of PM_{2.5}/PM₁₀ Variation based on Precipitable Water Vapor Wind Speed [J]. *Journal of Catastrophology*. **30** (1), 5, **2015**.
21. Ministry of Environmental Protection of China. The 12TH five-year environmental monitoring work manual. China Environmental Science Press. 292, China, **2012**.
22. DENG X., TANG Z. Moving Surface Spline Interpolation Based on Green's Function. *Mathematical Geosciences*. **43** (6), 663, **2011**.
23. WANG T., NIE W., GAO J., XUE L.K., GAO X.M., WANG X.F., QIU J., POON C.N., MEINARDI S., BLAKE D., WANG S.L., DING A.J., CHAI F.H., ZHANG Q.Z., WANG W.X. Air quality during the 2008 Beijing Olympics: secondary pollutants and regional impact. *Atmospheric Chemistry and Physics*. **10** (16), 7603, **2010**.